# Supplementary Material

## 1 OBSERVED AND PREDICTED SXR RADIANCES IN THE QUIET SUN

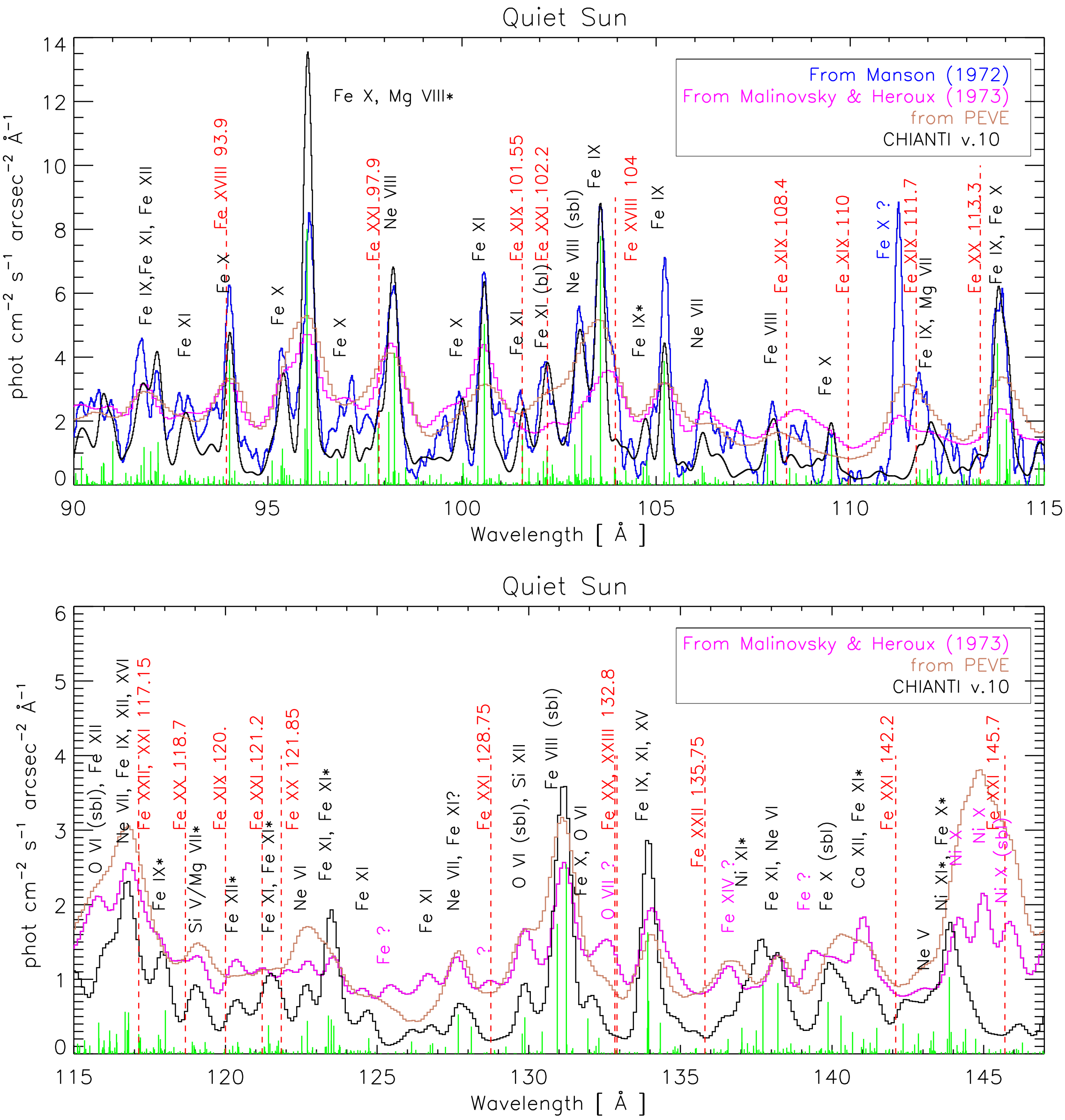


**Figure S1.** Predicted SXR quiet Sun radiances, obtained from the irradiance spectra of Manson (1972), Malinovsky and Heroux (1973), and prototype EVE (Woods et al., 2009), with over-plotted a simulated quiet Sun CHIANTI spectrum (black). The locations of the high-$T$ lines are shown in red. The main ions contributing to the CHIANTI lines are labelled, while all those contributing to the CHIANTI spectrum are shown in green. A few observed lines are missing in CHIANTI. Conversely, a few CHIANTI lines are not at the correct wavelengths. Those unidentified are labelled with an asterisk.

The SXR lines are clearly visible in irradiance spectra only for larger flares, due to the background radiation of the solar disk. To assess the visibility of the hot lines in active region cores, one would need

SXR radiance measurements, which are not available yet. We therefore need to rely on simulated spectra. As we have mentioned, the atomic data and line identifications in the whole SXR spectral region are not complete, so we do have a problem.

We therefore show in this Section a benchmark of the latest CHIANTI v.10 atomic data against two of the best soft X-ray medium-resolution full-Sun spectra, obtained with rocket flights in the 1960s: the quiet Sun spectrum from Manson (1972), available up to 115 Å, and the lower-resolution Malinovsky and Heroux (1973) irradiance spectrum. Both spectra were obtained from the published plots, and radiometrically recalibrated by Del Zanna (2012) using as a reference the 2008 April 14 irradiances from the prototype EVE instrument (Woods et al., 2009), when the Sun was at solar minimum.

We have converted the spectra to radiances assuming a limb-brightening increase of the average center-Sun radiances of a factor of 1.3 (Andretta and Del Zanna, 2014). The spectral resolution of the Manson (1972) spectra was about 0.2 Å (FWHM). The Sun probably had some flare emission during the flight of the Malinovsky and Heroux (1973) spectrum, as significant emission in Fe XVIII (94, 104 Å) was recorded. However, the bulk of the spectrum originated from the quiet Sun, as in the Manson (1972) case.

Fig. S1 shows a visual summary, with the observed spectra and the main lines in the two key SXR regions discussed here. There are some discrepancies between the Manson (1972) and Malinovsky and Heroux (1973) spectra, with the latter generally agreeing better with the lower-resolution PEVE.

Fig. S1 also shows a completely independent quiet Sun (QS) simulated spectrum, obtained from CHIANTI v.10, a $DEM$ obtained by Andretta et al. (2003) from SoHO CDS observations, and photospheric abundances. An instrumental FWHM of 0.25 Å was adopted for the 90–115 Å spectral range, while a FWHM of 0.5 Å was chosen for the comparison at longer wavelengths.

In some spectral regions, surprisingly good agreement between predicted and observed radiances is found. Further improvements will be achieved when the positions of the many unidentified lines is adjusted. The unidentified lines are noted with an asterisk in the Figure.

For the line identifications we have considered the Behring et al. (1972) line list, the literature from EBIT plasma (see, e.g. Lepson et al., 2002; Träbert et al., 2014), the Del Zanna (2012) identifications, B. Fawcett's plates for the iron ions, and other sources such as various compilations of laboratory measurements. We have also considered stellar spectra such as those discussed in Beiersdorfer et al. (2014), but note that the Manson (1972) solar spectra are far superior.

Clearly, the atomic data are still not complete, as discussed in detail in Del Zanna (2012). A few notable ions such as Ni X, still missing in CHIANTI, are noted. The key ions present in CHIANTI are marked in Fig. S1, although we note that many transitions (indicated with vertical green lines) generally contribute to the spectrum, at such medium resolution. Fig. S1 also shows in red the locations of the main hot lines, which mostly fall in regions relatively free of 'background' QS lines.

## 2 PREDICTED SXR RADIANCES IN AN ACTIVE REGION

The comparison in Fig. S1 gives us some confidence in presenting simulations of active region core spectra, in Figures S2,S3. We have used the $DEM$ and coronal abundances of an active region quiescent 3 MK loop, described in Del Zanna (2013) and shown in Figure 9 in that paper. We adopted, following our straw-man design, a pixel size of 0.01 Å and an instrumental width of 0.025 Å.

With the increased iron abundances by a factor of 3.2, there is an increased signal in most lines, compared to the quiet Sun case, which had photospheric abundances. Also, there is increased emission

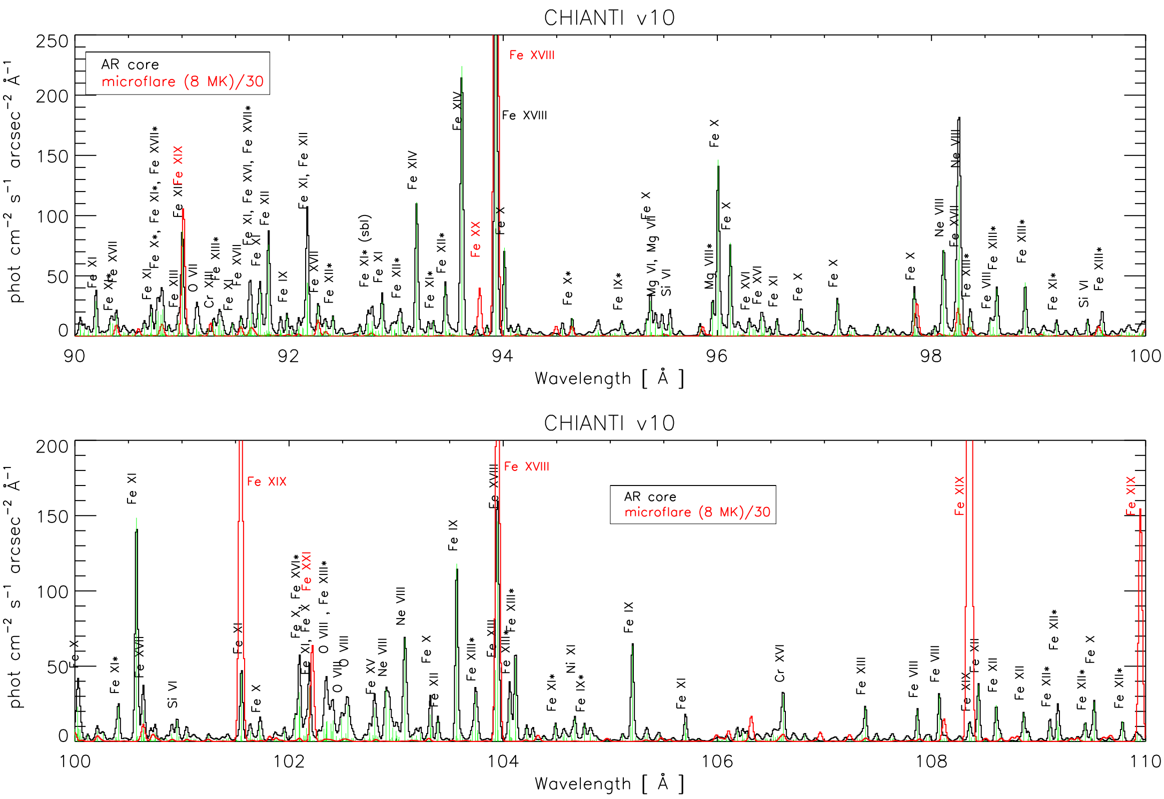


**Figure S2.** Simulated CHIANTI v.10 SXR spectra (90–110 Å) of the core of an active region, with over-plotted the spectrum of an A-class 8 MK microflare, reduced by a factor of 30. The lines contributing to the spectrum are shown in green, while the main ions are labelled. The unidentified lines are noted with an asterisk. The pixel size is 0.01 Å and the instrumental width is 0.025 Å.

in 2–3 MK spectral lines, especially in the Fe XVIII 104 Å line and several Fe XVI, Cr XVI, Si XII, Ca XII, Ca XIV, and Ca XV lines. The DEM was not constrained at 5-10 MK temperatures, and predicts a weak emission in the Fe XIX lines, which may or may not be present in actual AR spectra. On the other hand, we expect some emission from the Fe XVIII lines to always be present in AR observations.

A significant number of the weaker transitions are still not identified, hence their wavelengths could be off by 1 Å or more. They are noted with an asterisk in Figures S2,S3.

There are dozens of cool lines in the SXR, from ions such as Mg V, Mg VI, Mg VII, Mg VIII, O VI, O VII, O VIII, Si V, Si VI, Si VII, Ne V, Ne VI, Ne VII, Ne VIII, plus all ionisation stages of iron, from Fe VIII.

The Figures also over-plot in red the simulated A-class 8 MK microflare spectrum, reduced by a factor of 30. It is clear that most of the hot lines fall in region that are expected to be relatively free of blends. The Fe XVIII and Fe XIX microflare emission would be superimposed on the weak AR emission in the lines from these ions. A few hot lines are instead falling in regions where significant coronal 'background' emission is predicted to be present. However, we know from our previous Hinode EIS studies (see, e.g. Del Zanna et al., 2011; Mitra-Kraev and Del Zanna, 2019) that the lower-temperature coronal lines have little variations during the peak of a flare, so we expect that even the weakest hot lines will be easily detectable against the background.

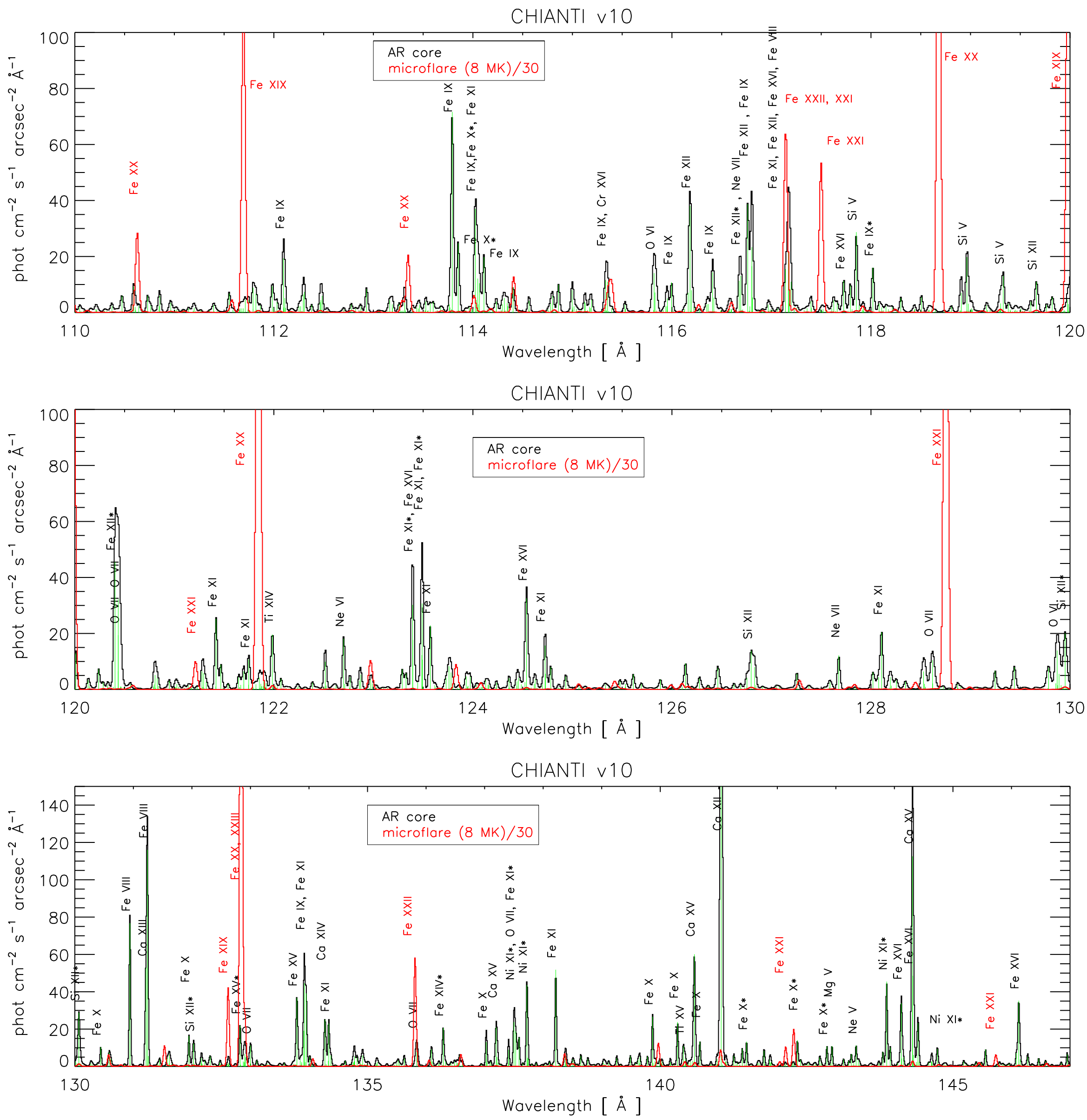


**Figure S3.** Same as Fig. S2 for the 110–147 Å spectral region.

## REFERENCES

Andretta, V. and Del Zanna, G. (2014). The EUV spectrum of the Sun: SOHO CDS NIS radiances during solar cycle 23. *A&A* 563, A26. doi:10.1051/0004-6361/201322841

Andretta, V., Del Zanna, G., and Jordan, S. D. (2003). The EUV helium spectrum in the quiet Sun: A by-product of coronal emission? *A&A* 400, 737–752

Behring, W. E., Cohen, L., and Feldman, U. (1972). The Solar Spectrum: Wavelengths and Identifications from 60 TO 385 Angstroms. *ApJ* 175, 493–+

Beiersdorfer, P., Lepson, J. K., Desai, P., Díaz, F., and Ishikawa, Y. (2014). New Identifications of Fe IX, Fe X, Fe XI, Fe XII, and Fe XIII Lines in the Spectrum of Procyon Observed with the Chandra X-Ray Observatory. *ApJS* 210, 16. doi:10.1088/0067-0049/210/2/16

Del Zanna, G. (2012). Benchmarking atomic data for astrophysics: a first look at the soft x-ray lines. *A&A* 546, A97. doi:10.1051/0004-6361/201219923

Del Zanna, G. (2013). The multi-thermal emission in solar active regions. *A&A* 558, A73. doi:10.1051/0004-6361/201321653

Del Zanna, G., Mitra-Kraev, U., Bradshaw, S. J., Mason, H. E., and Asai, A. (2011). The 22 may 2007 b-class flare: new insights from hinode observations. *A&A* 526, A1. doi:10.1051/0004-6361/201014906

Lepson, J. K., Beiersdorfer, P., Brown, G. V., Liedahl, D. A., Utter, S. B., Brickhouse, N. S., et al. (2002). Emission Lines of Fe VII-Fe X in the Extreme Ultraviolet Region, 60-140 Å. *ApJ* 578, 648–656. doi:10.1086/342274

Malinovsky, L. and Heroux, M. (1973). An Analysis of the Solar Extreme-Ultraviolet Between 50 and 300 A. *ApJ* 181, 1009–1030

Manson, J. E. (1972). Measurements of the Solar Spectrum between 30 and 128 Å. *Sol. Phys.* 27, 107–129. doi:10.1007/BF00151774

Mitra-Kraev, U. and Del Zanna, G. (2019). Solar microflares: a case study on temperatures and the Fe XVIII emission. *A&A* 628, A134. doi:10.1051/0004-6361/201834856

Träbert, E., Beiersdorfer, P., Brickhouse, N. S., and Golub, L. (2014). High-resolution Laboratory Spectra on the $\lambda$131 Channel of the AIA Instrument On Board the Solar Dynamics Observatory. *ApJS* 211, 14. doi:10.1088/0067-0049/211/1/14

Woods, T. N., Chamberlin, P. C., Harder, J. W., Hock, R. A., Snow, M., Eparvier, F. G., et al. (2009). Solar Irradiance Reference Spectra (SIRS) for the 2008 Whole Heliosphere Interval (WHI). *Geophys. Res. Lett.* 36, 1101–+. doi:10.1029/2008GL036373